Radio Science, Volume 6, Number 2, pages 299–304, February 1971

The formation by electric fields of field-aligned irregularities in the magnetosphere

C. G. Park and R. A. Helliwell

Radioscience Laboratory, Stanford University, Stanford, California 94305

(Received October 6, 1970.)

A possible mechanism for the formation of electron density irregularities in the magnetosphere is examined quantitatively. The mechanism involves localized $E \times B$ convection cells in which tubes of ionization with different total content are mixed. Under reasonable initial conditions, it is shown that a 0.1-mv/m electric field in the equatorial plane can produce electron density enhancements and depressions of the order of 5% at $L = 4$ in about one-half hour. These enhancements are large enough to trap whistler waves, whereas the depressions can trap HF waves. It is also shown that small-scale density irregularities can be produced by a much larger scale electric field. It is suggested that thundercloud electricity may be a possible source of the electric field responsible for the irregularities.

1. INTRODUCTION

In this paper a possible mechanism for the formation of field-aligned electron density irregularities in the magnetosphere is discussed. The mechanism involves a localized electric field in the magnetosphere which, together with the static geomagnetic field, causes localized convection of tubes of ionization according to the hydromagnetic relation $\mathbf{v} = \mathbf{E} \times \mathbf{B}/B^2$. The electric field has been suggested by several authors as the cause of field-aligned irregularities in the ionosphere [*Dagg*, 1957; *Reid*, 1965]. In this paper, we will present some results of a quantitative analysis of the formation of irregularities in the magnetosphere which are capable of ducting radio waves.

2. CALCULATIONS AND RESULTS

In this section, calculations will be made for a single convection cell under a particular set of conditions. The procedures to be followed are outlined below.

1. Assume an electrostatic field distribution in the equatorial plane in the magnetosphere to be turned on at time $t = 0$. The electric field remains constant for $t > 0$.
2. Compute the $(\mathbf{E} \times \mathbf{B})/B^2$ drift velocity from the assumed electric field distribution and a dipole geomagnetic field. With the assumption that magnetic field lines are equipotentials (i.e., 'frozen' field lines), the motion of tubes of ionization can be followed in time.
3. Assume an initial plasma distribution in the magnetosphere, and assume further that the plasma content in a tube of force above 1000-km altitude remains constant while the tube undergoes drift motion. The latter assumption will be discussed in section 4.
4. Compute the changes in the volume of tubes of force as they undergo drift.
5. With the results of step 4 and the assumption made in step 3, we compute the plasma density as a function of time and space.

Electrostatic field distribution. Figure 1 illustrates a simple electrostatic field distribution used in the calculations. The electric potential has a sinusoidal variation, with a wavelength of 600 km and an axial symmetry such that the equipotential lines are concentric circles as shown in the left half of the figure. The potential is assumed to be zero outside the 300-km radius. The corresponding electric field distribution is shown in the right half of the figure. The magnitude varies sinusoidally with the maximum field strength of 0.1 mv/m, and the direction is everywhere toward the center.

Imagine that the cell just described is placed in the magnetosphere such that the equipotential lines and the electric field vectors of Figure 1 lie in the equatorial plane and the center of the cell is at 4 earth radii from the center of the earth. The coordinate system is illustrated in Figure 2. In this coordinate system, the electric field can be expressed by

$$E = E_0 \sin (\pi r/A) \qquad \text{for} \quad r < A$$

where

$$E_0 = 10^{-4}\ v/\text{m} \qquad \text{and} \qquad A = 3 \times 10^5\ \text{m}$$

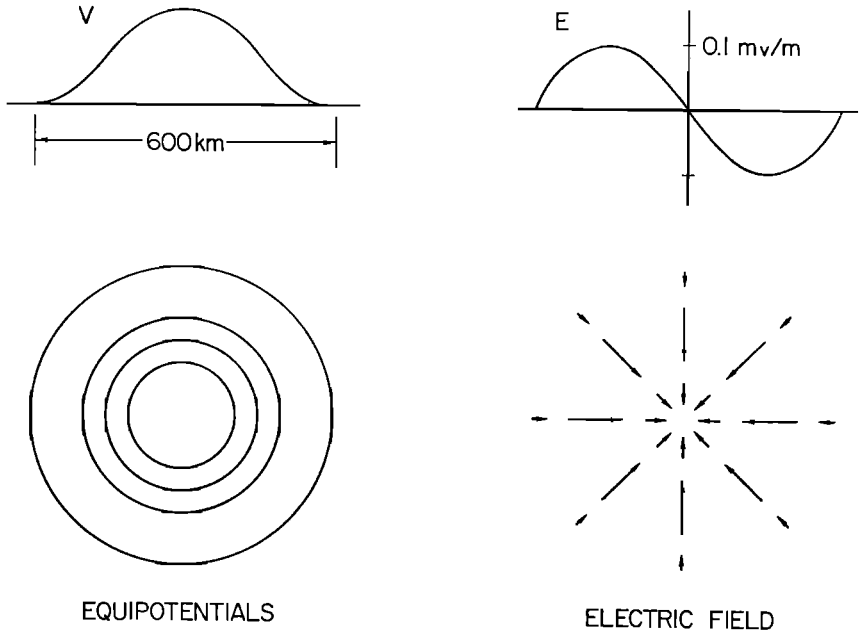

Fig. 1. Electric potential and corresponding electric field distribution.

The magnetic field is expressed by

$$B = B_0R_0^3(4R_0 + r\cos\phi)^{-3}$$

where R_0 is the earth's radius and B_0 is B at $R = R_0$.

Motion of tubes of ionization. Under the influence of the electric field assumed in the previous section and of the geomagnetic field, plasma motion in the equatorial plane is circular and follows the equipotential lines shown in Figure 1. The speed is $v_\phi = E/B$, or

$$v_\phi = \frac{E_0}{B_0R_0^3}(4R_0^3 + r\cos\phi)^3 \sin\left(\frac{\pi r}{A}\right)$$

The position of a tube of ionization in the equatorial plane can be found as a function of time by

$$r(t) = r_0 \tag{1}$$

and

$$\phi(t) = \phi_0 + \int_0^t \frac{v_\phi}{r_0}\,dt \tag{2}$$

where the subscript zero is used for the initial values at $t = 0$. The ionization off the equatorial plane moves in such a way that the same ionization always lies in a tube of force.

Figure 3 shows the motion of tubes of ionization in the equatorial plane. A number of test tubes of ionization initially at $\phi = 0$ are represented by a row of dots. Their positions at $t = 10$, 30, and 60 minutes are shown in the figure. In this simple model, the plasma at the center and on the circumference of the convection cell remains stationary while the plasma inside whirls about the center, forming a vortex. Owing to differential rotation, the tubes initially positioned along a straight line ($t = 0$) are later found along a spiral ($t = 60$ min). The spiral will be wound up tighter as time goes on.

Initial conditions. For the purpose of this calculation, tube content is defined as the total number of electrons in a tube of force above a unit cross-sectional area at 1000-km altitude, extending to 1000-km altitude in the conjugate hemisphere.

As an initial condition, we assume that tube con-

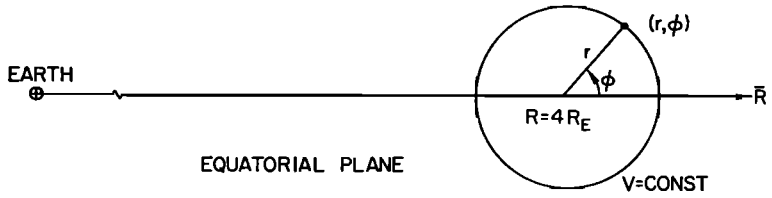

Fig. 2. The coordinate system used for calculations.

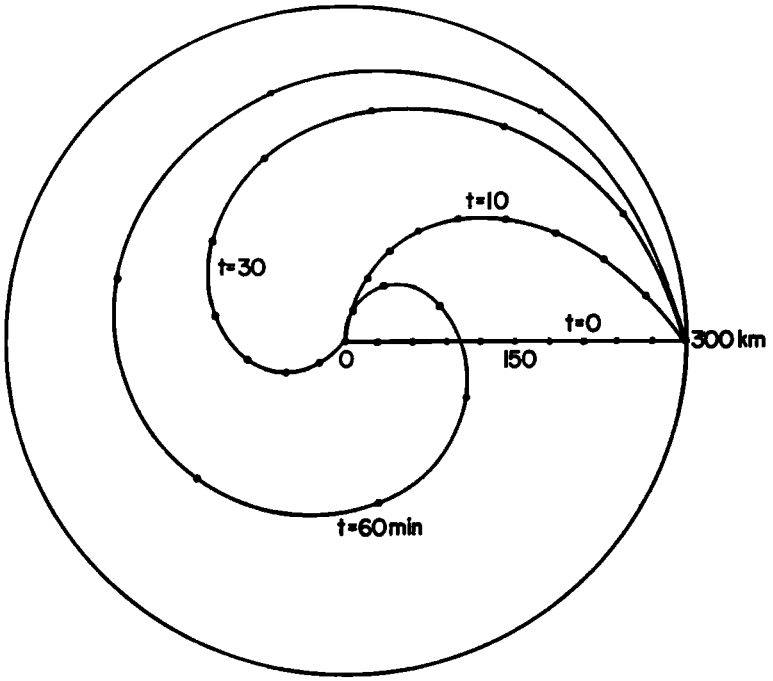

Fig. 3. A plot illustrating the motion of test tubes of ionization inside a convection cell. The dots indicate the equatorial crossing points of the tubes. The center of the convection cell is at $L = 4$, and the radius vector points to the right.

tent has no longitudinal or local time variations, but it increases 5% with every 300-km increase in equatorial radius. The initial tube content can then be expressed by

$$N_0 = N_4(1 + 0.05(r_0/A) \cos \phi_0) \qquad (3a)$$

where N_4 is the tube content at 4 R_E. The corresponding equatorial density profile can be computed from the tube content profile, if we assume diffusive equilibrium distribution of ionization along magnetic field lines. Electron density changes approximately inversely with the change in tube volume. Near $L = 4$, tube volume increases about 5% with every 300-km increase in equatorial radius (the same as the assumed tube content profile). The equatorial electron density is then expected to be approximately constant across the convection cell, provided there is no large variation in ion composition or temperature. The initial equatorial electron density is, therefore, taken to be constant across the convection cell.

Whistler observations have shown that tube content in the plasmasphere frequently increases with increasing L value, and large-scale electron density variations sometimes have the same characteristics as the initial profile assumed here [*Angerami and Carpenter*, 1966; *Park and Carpenter*, 1970].

Electron density variations. To calculate equatorial electron density $n_{eq}(r, \phi, t)$, we first find tube content $N(r, \phi, t)$ as follows. We trace the motion of the tube of force at (r, ϕ, t) backward in time to find its initial position (r_0, ϕ_0) by using equations 1 and 2. From the initial position and from equation 3, tube content $N_0(r_0, \phi_0)$ is found. Since the content of a drifting tube is assumed to remain constant,

$$N(r, \phi, t) = N_0(r_0, \phi_0) \qquad (3b)$$

The value of n_{eq} is then calculated from N; we assume diffusive equilibrium distribution along the field line.

Since the size of the convection cell (600-km diameter) is small compared to the distance from the earth ($4R_E$), the following simplifying approximations can be made. First, the ratio $N/n_{eq} \propto R^4$, second, changes in the cross-sectional area of a tube at 1000 km as it drifts around can be ignored, and, third, the vertical component of the plasma motion near the base of the tube can be ignored.

The results of the calculations are shown in Figure 4, in which the variations in tube content (top) and equatorial electron density (bottom) along the radius vector in the equatorial plane are shown at $t = 0$, 30, and 120 minutes. Both tube content and equatorial density are normalized to the values at $L = 4$, and the ordinates are in percentage. Figure 5 is a photograph of three-dimensional models showing the changes in equatorial electron density inside the convection cell as a function of time.

There are several features of the result to be

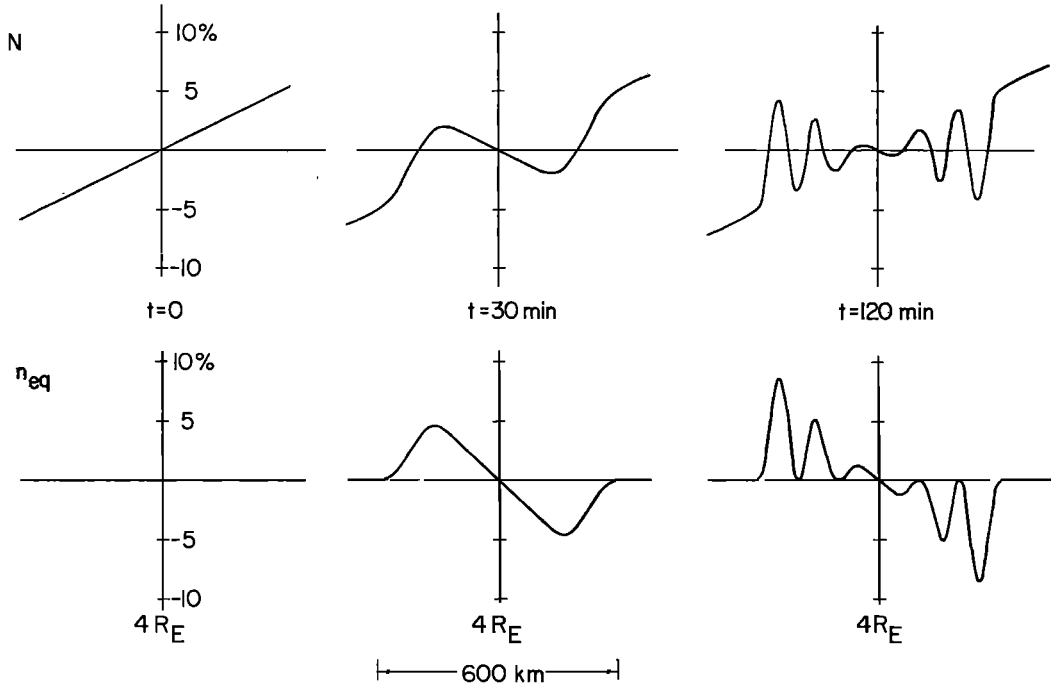

Fig. 4. Plots of tube content (top) and equatorial electron-density (bottom) variations across the convection cell of Figure 3, in the radial direction. Tube content and equatorial density are normalized to the values at $L = 4$. The profiles at three different times show the evolution of irregularities.

pointed out. According to *Smith* [1961] and *Angerami* [1970], whistler ducts are most likely to be enhancements of the order of 5%. On the other hand, observed conjugate HF ducts [*Muldrew*, 1967] would require depressions of the order of 1%. As can be seen in Figures 4 and 5, this mechanism can produce enhancements and depressions of order 5% at $L = 4$ in 30 minutes with 0.1 mv/m electric field in the equatorial plane and reasonable initial conditions. Since this mechanism does not add or subtract plasma from the magnetosphere, but merely stirs up the existing plasma, an enhancement can be produced only at the expense of a depression somewhere else.

At $t \sim 60$ minutes, multiple peaks and valleys start to appear, and the electron density profile becomes more complex. At $t = 120$ minutes, the dimension of peaks and valleys is ~50 km, and the difference between peak and valley densities is limited only by the maximum variation in initial tube content across the convection cell, which is 10%. It is very significant that small-scale electron density irregularities can be produced by a much larger scale electric field. This point will be discussed further in the next section.

From this analysis we can see that the evolution of irregular structures, as illustrated in Figures 4 and 5, depends on the shape, but not the amplitude, of the electric field distribution. Thus if we double the field of Figure 1, the same evolution of structures would proceed at twice the speed.

3. POSSIBLE SOURCES OF ELECTRIC FIELD

Several authors have suggested possible sources of electrostatic field in the magnetosphere and the ionosphere which could produce field-aligned density irregularities. *Dagg* [1957] suggested turbulent wind in the dynamo region as the source of the electric field that may be responsible for the *F*-region irregularities. *Reid* [1965] suggested turbulence in the magnetosphere as the source of the electric field. *Cole* [1970] suggested asymmetric wind in the conjugate dynamo region. In this paper, we suggest that thundercloud electricity is a possible source of the electric field in the magnetosphere, and some quantitative arguments are presented below.

In section 2, it was shown that 0.1-mv/m field strength in the equatorial plane could produce a whistler duct at $L = 4$ in 30 minutes. This corresponds to ~1 mv/m at *F*-region heights, if we assume equipotential magnetic field lines. According to *Spreiter and Briggs* [1961], an electric field of the

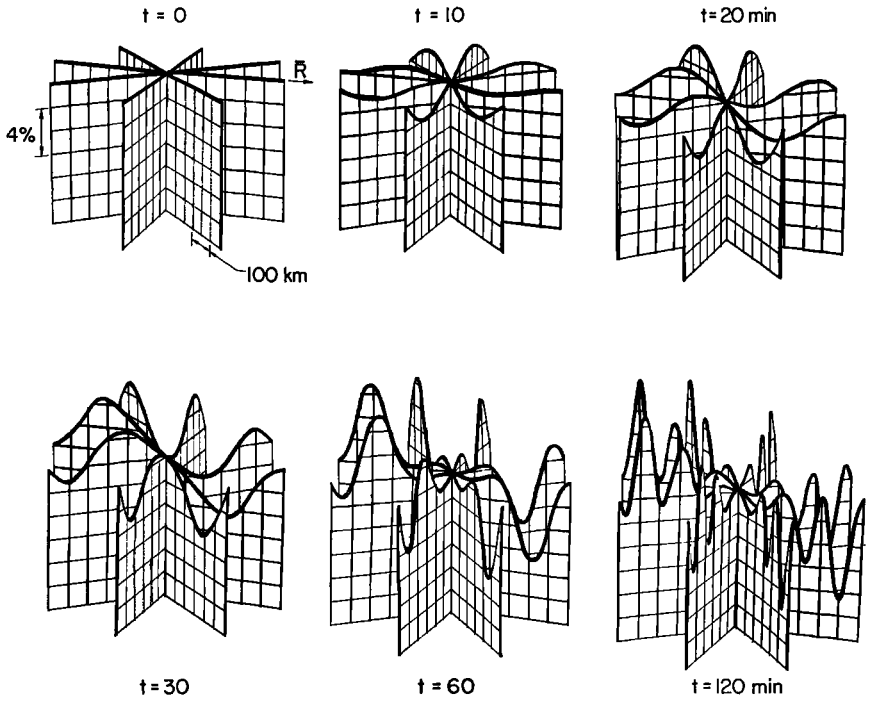

Fig. 5. A photograph of three-dimensional models of equatorial electron density inside the convection cell of Figure 3. The direction of the radius vector is indicated by an arrow.

dimensions of interest here (wavelength of ~50 km in the ionosphere) can be mapped from the 100-km level to the *F* region with a reduction in amplitude by a factor of less than 10. The electric field of section 2 then corresponds to ~10 mv/m at 100-km altitude. The thundercloud electric field may be 10^6 v/m at 20-km altitude (cloud-to-cloud discharges have been observed at altitudes above 10 km [*Taylor*, 1969]). If thundercloud electricity is to produce a whistler duct in about one-half hour, the attenuation of electric field between the altitudes of 20 and 100 km must not exceed ~10^8. If the attenuation is larger, more time is required to form the duct in proportion to the attenuation.

The attenuation is closely related to the height variation of conductivity and to the wavelength of the electric field. A simple analysis of a three-dimensional boundary value problem involving scalar conductivity that increases exponentially with altitude with a constant scale height has been made. The results show that the attenuation of an electric field with 100-km wavelength in both east-west and north-south directions (this roughly corresponds to the size of the convection cell in section 2) is ~10^7 — 10^{10} for conductivity scale heights of 6–4 km. Calculations involving more realistic conductivity models (i.e., *Cole and Pierce* [1965]) require numerical techniques, and the results will be presented in a future report.

It is not possible to evaluate the relative importance of various sources of electric field on a quantitative basis, because no measurements or theoretical calculations of the electric field strength are now available. In mapping electric fields in the lower atmosphere, the ionosphere, and the magnetosphere, we have found that the attenuation is closely related to the wavelength, so that small scale electric fields have a limited region of influence. This was pointed out by earlier workers [*Spreiter and Briggs*, 1961; *Reid*, 1965; *Mozer and Serlin*, 1969]. In searching for the source of electric fields, however, it should be borne in mind that small-scale irregularities can be produced by a much larger scale electric field, as was demonstrated in section 2.

4. DISCUSSION

In section 2, the initial tube content was assumed to have a gradient only in the radial direction. If the gradient has a different direction, the results would be similar to those of Figures 4 and 5, except that they would be rotated by an appropriate angle. Large longitudinal variations in electron density in the magnetosphere have been reported by *Park and Carpenter* [1970] and *Bullough and Sagredo* [1970].

If the initial tube content is uniform in both longitude and latitude (this corresponds to equatorial electron density varying as $\sim R^{-4}$ in radial direction and remaining constant in longitude), mixing of tubes does not produce any changes in electron density as long as the content of the drifting tubes remains constant. In the first order, some spatial variation in tube content is a necessary initial condition for producing density irregularities. However, the assumption of content-preserving drift is not strictly true. A drift motion in latitude has a vertical component at ionospheric heights, which alters the coupling conditions between the magnetospheric tube of ionization and the underlying ionosphere. As a result, tube content will change somewhat through diffusion along field lines [*Park,* 1970]. In the second-order picture, then, any localized convection activity is expected to produce irregularities regardless of initial conditions. Irregularities, however, should be more difficult to form in regions where tube content is uniform.

Another factor of importance is the diffusion of ionization out of a duct. This is a difficult problem and will not be considered in detail here. However, a first-order consideration of the problem suggests that a lifetime of several days can be expected. Consistent with this estimate are observations of whistlers showing that individual whistler components, corresponding to separate ducts, often retain their identity for several hours [*Carpenter,* 1966; *Park and Carpenter,* 1970].

We recall that, in section 2, a very complex structure in electron density evolved from a very simple initial condition and a very simple static electric field distribution. If the electric field and the initial conditions were more complex, or if the electric field varied with time, the result would be correspondingly more complex. There may be many convection cells with different electric field sources, some of which may overlap or interact with each other. Under such circumstances, the magnetosphere is expected to have very complex filamentary structures.

5. CONCLUSIONS

The results of this study are summarized as follows. First, under reasonable initial conditions, a 0.1-mv/m electric field in the equatorial plane can produce a whistler duct at $L = 4$ in about 30 minutes. Second, small-scale irregularities can be produced by a much larger scale electric field. Third, this mechanism produces both enhancements and depressions in electron density. And fourth, thundercloud electricity is suggested as a possible source of the electric field in the magnetosphere which produces irregularities.

Acknowledgment. This research was supported by the National Science Foundation, Section on Atmospheric Sciences, under grant GA-18126.

REFERENCES

Angerami, J. J. (1970), Whistler duct properties deduced from VLF observations made with the Ogo 3 satellite near the magnetic equator, *J. Geophys. Res., 75,* 6115–6135.

Angerami, J. J., and D. L. Carpenter (1966), Whistler studies of the plasmapause in the magnetosphere, 2, Electron density and total tube electron content near the knee in magnetospheric ionization, *J. Geophys. Res., 71,* 711–725.

Bullough, K., and J. L. Sagredo (1970), Longitudinal structure in the plasmapause: VLF goniometer observations of knee-whistlers, *Nature, 225,* 1038–1039.

Carpenter, D. L. (1966), Whistler studies of the plasmapause in the magnetosphere, 1, Temporal variations in the position of the knee and some evidence on plasma motions near the knee, *J. Geophys. Res., 71,* 693–709.

Cole, K. D. (1970), Formation of field-aligned irregularities in the magnetosphere, paper presented at Upper Atmospheric Currents and Electric Fields Symposium, Boulder, Colorado, August 17–21.

Cole, R. K., Jr., and E. T. Pierce (1965), Electrification in the earth's atmosphere for altitudes between 0 and 100 kilometers, *J. Geophys. Res., 70,* 2735–2749.

Dagg, M. (1957), The origin of the ionospheric irregularities responsible for radio-star scintillations and spread-*F*, 2, Turbulent motion in the dynamo region, *J. Atmos. Terr. Phys., 11,* 139–150.

Mozer, F. S., and R. Serlin (1969), Magnetospheric electric field measurements with balloons, *J. Geophys. Res., 74,* 4739–4754.

Muldrew, D. B. (1967), Medium frequency conjugate echoes observed on topside-sounder data, *Can. J. Phys., 45,* 4935–4944.

Park, C. G. (1970), Electric fields as the cause of nighttime increases in electron concentration in the mid-latitude ionospheric *F* region, paper presented at Upper Atmospheric Currents and Electric Fields Symposium, Boulder, Colorado, August 17–21.

Park, C. G., and D. L. Carpenter (1970), Whistler evidence of large-scale electron-density irregularities in the plasmasphere, *J. Geophys. Res., 75,* 3825–3836.

Reid, G. C. (1965), Ionospheric effects of electrostatic fields generated in the outer magnetosphere, *Radio Sci., 69D,* 827–837.

Smith, R. L. (1961), Propagation characteristics of whistlers trapped in field-aligned columns of enhanced ionization, *J. Geophys. Res., 66,* 3699–3707.

Spreiter, J. R., and B. R. Briggs (1961), Theory of electrostatic fields in the ionosphere at polar and middle geomagnetic latitudes, *J. Geophys. Res., 66,* 1731–1744.

Taylor, W. L. (1969), Determining lightning stroke height from ionospheric components of atmospheric waveforms, *J. Atmos. Terr. Phys., 31,* 983–990.